Colloid Polym Sci (2011) 289:1579–1587
DOI 10.1007/s00396-011-2482-0

ORIGINAL CONTRIBUTION

Synthesis and properties of new polymeric surfactant with quaternary ammonium salt

Lei Zhang · Xin Lv · Yuejun Zhu · Jian Zhang · Hong Wang · Yebang Tan

Received: 18 April 2011 / Revised: 17 June 2011 / Accepted: 4 July 2011 / Published online: 20 July 2011

Abstract The polymeric surfactant with quaternary ammonium salt (PQ) was synthesized by cationic ring-open polymerization using boron trifluoride diethyletherate as cationic catalyst. The chemical structure and aggregation behavior of PQ were studied by ^{1}H NMR, surface tension, static light scattering, dynamic laser light scattering, electrical conductivity, and fluorescence measurement. The results show the surface tension (γ_{cmc}) and critical micelle concentration (cmc) of PQ decrease with increasing of sodium chloride concentration. The cmc and γ_{cmc} values of PQ measured by electrical conductivity and fluorescence measurements mainly identify with that obtained by surface tension measurements. The thermodynamic parameters (ΔG_m^0,ΔH_m^0,ΔS_m^0) from electrical conductivity indicated that the micellization of PQ was mainly the process of entropy-driven. In addition, the results from the viscosity stability between hydrolyzed polyacrylamide (HPAM) and PQ showed that the viscosities of mixed system for HPAM and PQ are higher than the viscosity of HPAM.

L. Zhang · H. Wang · Y. Tan (✉)
School of Chemistry and Chemical Engineering,
Shandong University,
Jinan 250100, People's Republic of China
e-mail: ybtan@sdu.edu.cn

L. Zhang · H. Wang · Y. Tan
Key laboratory of Special Functional Aggregated Materials,
Shandong University, Ministry of Education,
Jinan 250100, People's Republic of China

X. Lv · Y. Zhu · J. Zhang
Technology Research Department CNOOC Research Center,
State Key Laboratory of Offshore Oil Exploitation,
Beijing 100027, People's Republic of China

Keywords Polymeric surfactant · Quaternary ammonium salt · Water-soluble polymer aggregation behavior · Viscosity stabilizer

Introduction

Surfactants with quaternary ammonium salt, which are of high surface activity, good adsorption, flocculation properties, compatibilization properties, antistatic performance, antibacterial properties, and good detergency, are widely used in the fields of new technology such as manufacture, life science and biotechnology, nanomaterials, cosmetic industry, detergents, petroleum industry, and so on [1–10]. This kind of surfactants consisting of an ionized nitrogen atom and a positive charge, which is compensated with counterions, is the important symbol, and the molecule from the molecule structure can be divided into the hydrophilic and hydrophobic cationic long chains. Surfactants for quaternary ammonium salt exist in the form of dimers, oligomers, or polymers [3, 7, 9, 11–20]. Compared to the general monomeric quaternary ammonium salt, polymeric surfactants with quaternary ammonium salt (PQ) are synthesized from the monomer of surfactant with polymerizable groups, such as double bond, epoxy group and so forth, either at the polar head or at the polar tail [13, 21–23].

The interactions of water-soluble polymers and ionic surfactants in aqueous solution are of interest from the fundamental standpoint of special structure and dynamics of polymer/surfactant association and can be used in the process of enhanced oil recovery (EOR). The ability of surfactants to aggregate and form micelles adds a particular dimension to their interactions with water-soluble polymers [24–33]. One of the most widely used water-soluble polymers is hydrolyzed polyacrylamide (HPAM). In the application of HPAM in oil fields, it is of primary

importance to make sure that the polymer solutions remain effective and stable over long periods of time at elevated temperatures. Some literature data are concerned with the effect of temperature on HPAM solution stability; additives or purging with nitrogen are used to prevent oxygen and thermal degradation [34]. According to some reported literature, cationic surfactant containing quaternary ammonium salt is an effective additive agent from polymer flooding in the EOR, which can be used as viscosity stabilizer [24, 26, 29].

In this work, we synthesized a new PQ by utilizing cationic ring-open polymerization (boron trifluoride diethyletherate catalysis) [35–38], where the monomer for epoxy compound was first synthesized by quaternization reaction [39]. This kind of polymeric surfactant, which presents a new structure and properties, has been hardly reported. Besides, the stability between HPAM and PQ in the solution was investigated by the methods of viscosity measurements and dynamic light scattering measurements in order to study the salt resistance and viscosity stability of mixed system.

Experimental

Materials

6-Bromo-1,2-expoxyhexane was purchased from Shijiazhuang Haotian Chemical Co.; N,N-dimethylhexadecylamine was obtained from Feixiang Chemicals (Zhangjiagang) Co.; boron trifluoride diethyletherate ($BF_3{\cdot}OEt_2$), pyrene (Alfa-Aesar Regent Co.) was recrystallized from alcohol; tetrahydrofuran (chromatographic pure, THF) was purchased from J&K Scientific Ltd.; hydrolyzed polyacrylamide (HPAM, molecular weight was 1.2×10^7 g/mol; degree of hydrolysis was 18%) was obtained from Technology Research Dept. CNOOC Research Center. Boron trifluoride diethyletherate and dichloromethane were purified by distilled over CaH_2 and other solvents were stored at over 4A molecular sieves. Deioned water was used to prepare the aqueous solution in all experiments.

Synthesis of n-cetyldimethylamine-1,2-expoxyhexyl ammonium bromide

The epoxide quaternary ammonium salt was prepared by quaternization reaction. A 100 mL three-neck round-bottom flask equipped with mechanical stirrer and condenser pipe was used for the synthesis in a nitrogen atmosphere. A 2.71 g (0.01 mol) N,N-dimethylhexadecylamine was completely dissolved in 20 mL acetone. After that, 1.97 g (0.011 mol) 6-bromo-1,2-expoxyhexane was added, stirred, and purged with nitrogen. The quaternization reaction was allowed to proceed under continuous stirring for 24 h at 50 °C. After the reaction finished, the product was concentrated and washed by absolute ether. The purified product was recovered and dried several days under vacuum, and the field of product was 92%. The schematic diagram of synthesis route is presented in Fig. 1.

Synthesis of PQ

PQ was obtained by cationic ring-open polymerization. Polymerizations were carried out at room temperature (25 °C) in a glass 100-mL two-neck round-bottom flask with a mechanical stirrer and N_2 inlet/outlet. This reactor was dried and vacuumized through a vacuum and gentle stream of dry nitrogen in order to make better conducive to the polymerization. A 4.48-g (0.01 mol) monomer that was obtained by the above preparation methods and 25 mL dichloromethane were added into the reactor under N_2 atmosphere. The catalyst 600 μL $BF_3{\cdot}OEt_2$ ([M]/[cat.]= 5) was introduced into the reaction system using a microsyringe. After 24 h, the polymerization was terminated by adding trace water. The solution was concentrated under reduced pressure and washed by absolute ether. The polymer was recrystallized and dried several days under vacuum and the field of product was 90%. The schematic diagram of synthesis route is presented in Fig. 2.

The evaluation of viscosity stability for mixed system between HPAM and PQ

The fixed concentration of HPAM (1,200 mg/L) with the different concentration of PQ (0, 15, 25, 35, and 50 mg/L) were dissolved in the simulated water, which the salinity of simulated water was 2,743 mg/L and contained 1,201.2 mg/L NaCl, 3.775 mg/L KCl, 130.45 mg/L $CaCl_2$, 24.54 mg/L $MgCl_2$, 137.7 mg/L Na_2SO_4, 81.58 mg/L Na_2CO_3, 1163.9 mg/L $NaHCO_3$. After sheared 20 s in order to simulate the process of site application, the mixed systems were placed under the temperature (58 °C) for simulating the temperature of oil layer and carried on the aging experiment.

Characterization

^1H NMR experiments were performed on a Bruker ADVANCE 400 spectrometer. $CDCl_3$ was used for field-

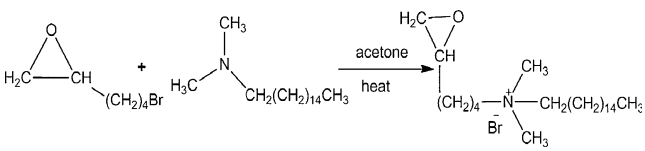

Fig. 1 Synthesis of monomer

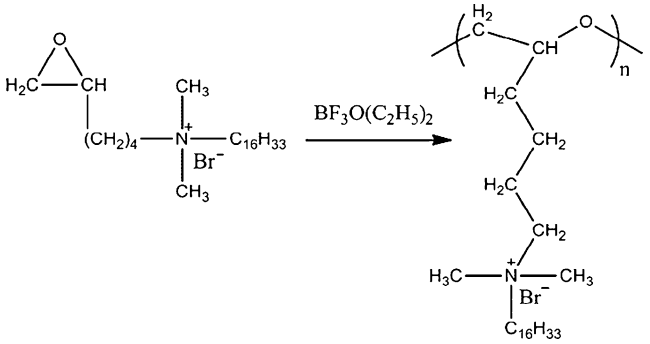

Fig. 2 Synthesis of PQ

frequency lock, and the observed ^{1}H chemical shifts were reported in parts per million (ppm) relative to an internal standard.

Surface tension (γ) was measured on Processor Tension K100 (Krüss Company, Germany) using the ring method. Surfactant solutions were kept for 15 min to equilibrate. All the measurements were performed at 25.0±0.1 °C.

Static light scattering (SLS) was performed with a DAWN HELEOS light scattering instrument (Wyatt Technology) equipped with a linearly polarized gallium arsenide (GaAs) laser (λ=658 nm) at 25 °C. The laser was positioned so that the incident beam was vertically polarized. Zimm plots were obtained using Astra software. The polymeric surfactant were examined in benzylmagnesium chloride solution and filtrated with a 0.2-μm Millipore filter. A differential refractive index detector (Optilab-REX) was used to measure the refractive index (dn/dc) of the polymeric surfactant.

Dynamic light scattering (DLS) measurements were carried out on a multiangle laser photometer equipped with a linearly polarized gallium arsenide (GaAs) laser (λ= 658 nm; Wyatt Technology Co. DAWN HELEOS) at 25 °C. The scattering angle is 90°. The polymeric surfactant were dissolved in ultrapure water whose electric conductivity was 18.25 mΩ cm, and filtrated through a 0.8-μm Millipore filter before the DLS measurements.

Fluorescence spectra were measured by a Hitachi F-4500 fluorescence spectrophotometer using 1.0-cm quartz cell. Pyrene spectra were recorded with fixed excitation wavelength at 335 nm, and the slit widths of excitation and emission were fixed at 2.5 and 5 nm, respectively. The emission spectra were scanned at the range of 350–500 nm. I_1 and I_3, which was fluorescence intensity, were taken from the emission intensities at 373 and 384 nm, and the ratio of I_1/I_3 was used to estimate the micropolarity sensed by the pyrene as well as to obtain the critical micelle concentration of the surfactants in aqueous solution at 25 °C. The pyrene concentration was fixed at 1.0×10^{-6} mol/L in the measurements.

Electrical conductivity of the polyether surfactant solutions was carried out on a function of concentration with a low-frequency conductivity analyzer (model DDS-307, Shanghai Precision & Scientific Instrument Co.) at five different temperatures for the PQ in aqueous solutions. All the measurements were repeated three times at each temperature.

The viscosity of mixed system between HPAM and PQ was measured by Brookfield DV-II viscometer (with low viscosity adapter accessories, rotor ULA) at 25 °C, and the rotate speed was fixed at 6 r/min (7.34 s^{-1} for shear rate).

Results and discussion

Characterization

Figure 3a shows the ^{1}H NMR spectra of n-cetyldimethylamine-1,2-expoxyhexyl ammonium bromide. In Fig. 3a, six characteristic peaks at 0.89, 2.49, 2.75, 3.41, 3.50, and 3.65 ppm that were ascribed to the corresponding hydrogen protons were labeled l, a, b, g, h, f; the peaks at 1.25–1.36 ppm were labeled k; the peaks at 1.60–1.89 ppm were labeled e, i, c, d, j. Figure 3b is the spectrum of polyester quaternary ammonium salt. The peaks at 0.89, 1.25–1.34, 3.14, and 3.85 ppm belong to l, k, g and f, respectively; the peaks at 1.55–1.69 ppm were labeled e, i, c, d, j; the peaks labeled as h, b, and a were ranged from 3.30 to 3.6 ppm. Compared with (A) and (B), the peaks labeled as a and b in Fig. 3a disappear in Fig. 3b, so that it is certain that the cationic ring-open polymerization was completed successfully.

The molecular weight of polymer was measured by SLS. Molecular weight (M_w), the second virial coefficient (A_2), and the mean square radius (R_g^2) of polymer chain were determined from the Zimm plot [40–42] on the basis of the equation as follows:

$$\frac{Kc}{R(\theta)} = \frac{1}{M_w}\left[1 + \frac{1}{3}q^2\left\langle R_g^2\right\rangle_z\right] + 2A_2c$$

In equations $K = 4\pi^2 n_0^2(\mathrm{dn/dc})^2/\left(N_A\lambda_0^4\right)$, and $q = (4\pi n_0/\lambda_0)\sin(\theta/2)$,

dn/dc is the increment of refractive index with concentration, n_0 is the refractive index of the solvent, N_A is Avogadro's number, λ_0 is the wavelength of the laser light in the solvent, and θ is the scattering angle. $R(\theta)$ is the difference in the Rayleigh ratio between the sample and the solvent (THF).

The molecular weight of PQ was performed in the THF solution. The value of dn/dc is 0.0730 for PQ in the THF solution. Figure 4 shows a static Zimm plot of polymeric surfactant in THF solution, where the concentration ranges

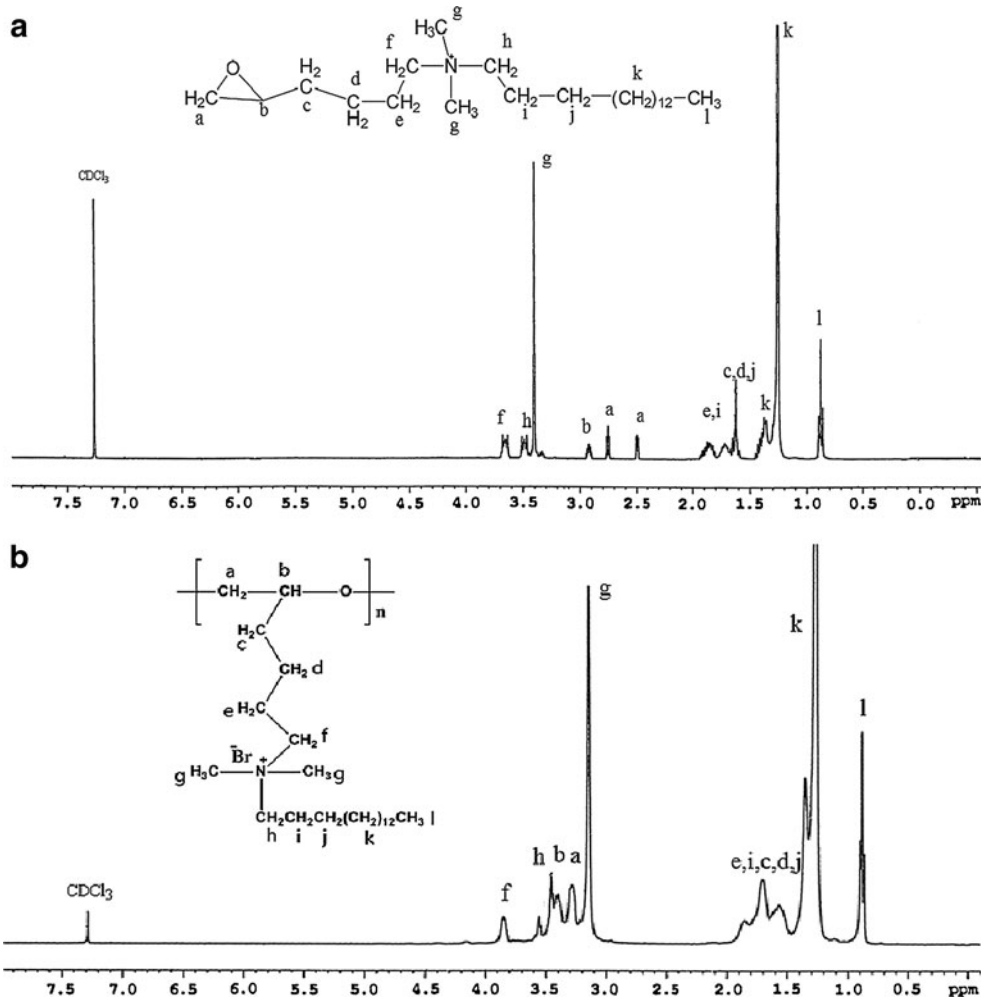

Fig. 3 ^{1}H NMR spectra of (**a**) monomer, (**b**) PQ in $CDCl_3$

from 5×10^{-4} to 1.5×10^{-2} g/mL. By using the projection $\theta=0$ and $C=0$, the values of Mw, and A_2 calculated in the equation were Mw$=1.292\times10^{4}$ g/mol, $A_2=4.187\times10^{-3}$ mol mL/g^2. The second virial coefficient (A_2) is always positive, indicating that THF solution is a good solvent for PQ.

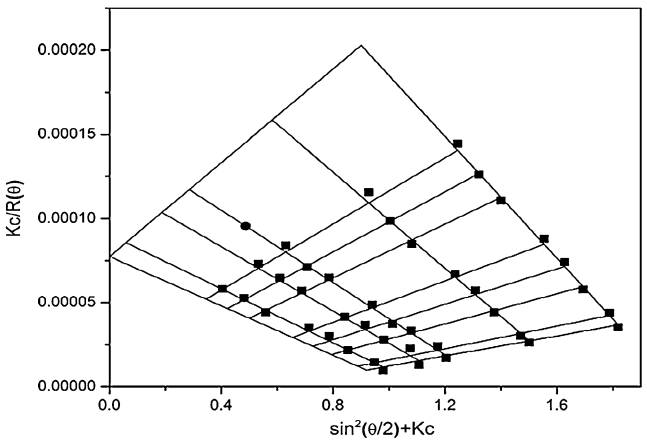

Fig. 4 Zimm plot for PQ in the THF solution

Surface tension

The relationship between the surface intension and the concentration of PQ in the presence of sodium chloride at 25 °C is shown in Fig. 5. It is clear that the relationship between surface tension and concentration of PQ is characterized by two distinguishable regions, one at the lower concentration range characterized by a fast decrease in the surface tension values, the other at the higher concentrations, in which the surface tension values remain almost constant. The concentration at the break point that separates the two regions is regarded as the critical micelle concentration (cmc).

The values of cmc and γ_{cmc} for polymeric surfactant in the different concentration of sodium chloride are listed in Table 1. The γ_{cmc} and cmc values of PQ decrease with the increase of the concentration of sodium chloride. The results may be explained as follows. The PQ forms ionic monolayer at the air/water interface, while the addition of electrolyte anions leads to the reduction of the thickness and potential of the electric double layer at the interface because of the electrostatic interaction between opposite charges. As a

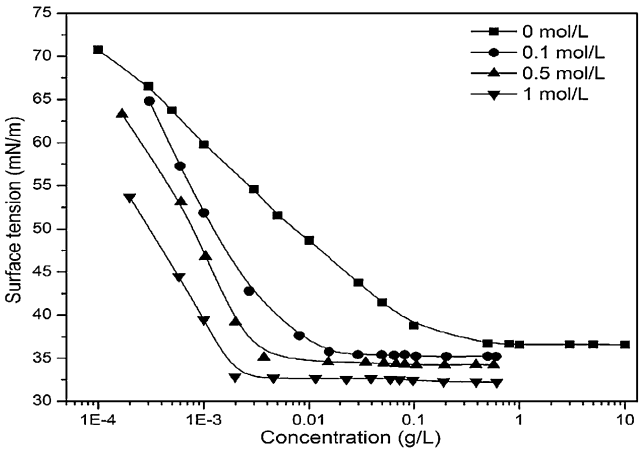

Fig. 5 Surface tension isotherms of PQ at different concentration sodium chloride solutions at 25 °C

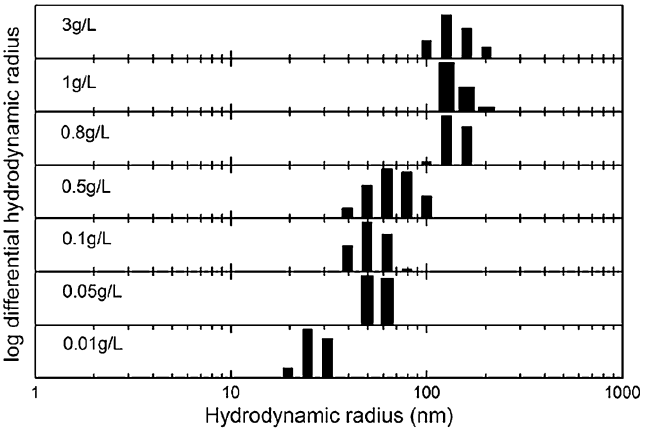

Fig. 6 Hydrodynamic radius distribution of PQ in the aqueous solution at different concentration at 25 °C

result, it induces the screening of the electrostatic repulsion among the polar head groups and leads to remarkably lower cmc and surface tension in comparison with the salt-free system [4]. More higher the concentration of NaCl gets, more obvious the reduction of cmc and surface tension becomes.

Dynamic light scattering

The distribution of the hydrodynamic radius (R_h) of PQ in the aqueous solution obtained by DLS is shown in Fig. 6. A distribution of the average R_h is observed when the polymeric surfactant concentrations are arranged from 0.01 to 3 g/L. The polymeric surfactants of lower concentration indicate smaller radius distribution (R_h<100 nm), while the radius distribution becomes larger along with the increase of the polymeric surfactant concentration, until the average R_h distribution gradually changed little with the increase of concentration. From Fig. 6, we can know that the polymeric surfactants in the aqueous solution have a very strong propensity to aggregate and form big size aggregates, so that the distributions of average R_h also increase. The changes of the R_h distribution basically identify with the variations of surface tension.

Fluorescence spectra

The fluorescence measurement for PQ was investigated by fluorescence spectrum using the pyrene probe. The intensity ratio of the first to the third peaks, I_1/I_3, is often used as a measure of the polarity of the microenvironment [43–46]. When surfactant self-assembly forms, pyrene molecules can get into the interior hydrophobic domain of surfactant micelles in the water, thus this will result in an abrupt change of the I_1/I_3 ratio, and the concentration corresponding to this abrupt change is the cmc. Figure 7a presents the fluorescence intension of pyrene probe for the polymeric surfactant in the aqueous solution at 25 °C. It is found that the fluorescence intension gradually becomes strong as the concentration of polymeric surfactant increases, which illustrate that the pyrene probe can be better dissolved in the micelle increasing the concentration of polymeric surfactant. The higher the concentration of polymeric surfactant is, the better the pyrene probe can be dissolved in the micelle and the stronger fluorescence intension becomes.

Figure 7b represents the I_1/I_3 ratio variation with the concentration. The cmc values at the inflection point are 0.35 g/L for the surfactant PQ, which is in accordance with the data obtained from surface tension. As shown in Fig. 7b, the systems contained pyrene, and polymeric surfactant has lower I_1/I_3 above the cmc, which the I_1/I_3 value is 1.02. The low I_1/I_3 value indicates that pyrene is solubilized in the palisade layer near the polar head groups for all the polymeric surfactant micelles in the aqueous solution.

Table 1 cmc and γ_{cmc} in the presence of sodium chloride

Concentration (mol/L)	cmc (g/L)	γ_{cmc} (mN/m)
0	0.36	36.6
0.1	0.015	35.4
0.5	0.0038	34.5
1	0.0018	32.6

Electrical conductivity

The changes of conductivity (κ) as a function of PQ concentration are shown in Fig. 8 at various temperatures. The cmc of polymeric surfactant estimated from electrical conductivity plots at different temperatures are listed in Table 2. It can be seen that the cmc values increase with raising the temperature, and the cmc values measured by electrical conductivity at 25 °C, are in accordance with those by surface tension. The degree of

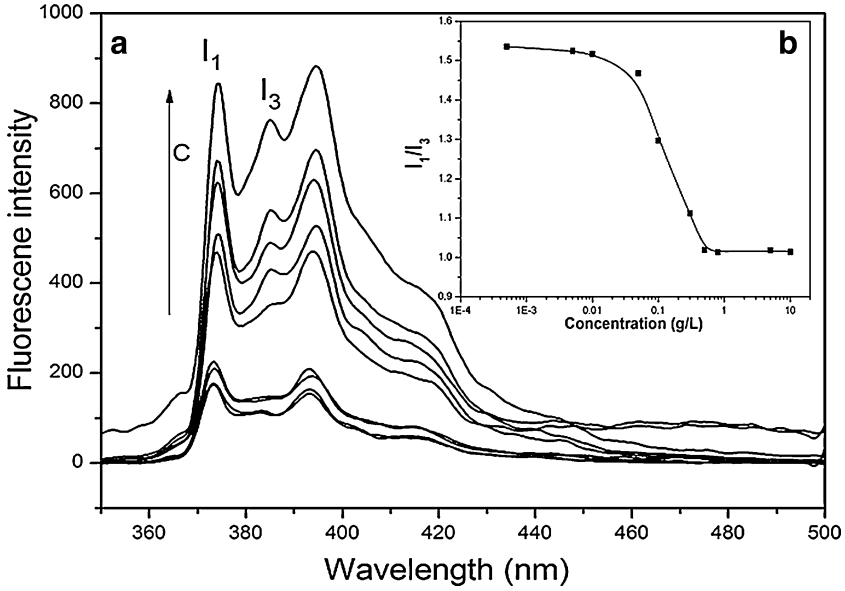

Fig. 7 **a** Fluorescence intension of pyrene probe for PQ **b** I_1/I_3 ratio of pyrene as a function of concentration for PQ

counterion dissociation, α, can be obtained from the ratio of the slopes above and below the cmc, while the degree of counterion binding to micelle, β, is $(1-\alpha)$. The β values at various temperatures are also listed in Table 2. As can be clearly seen from Table 2, the β values of PQ decrease with the increase of temperature, indicating that the combination of counterion and micelle surface is an exothermic process, which also reflects the combination of them, is done by static electricity between opposite charges.

The phase separation model is applied to compute the thermodynamic parameters of micellization, and the standard Gibbs free energy change of micellization can be calculated from the following equation [47–49]:

$$\Delta G_{\mathrm{m}}^{0} = RT(0.5+\beta)\ln X_{\mathrm{cmc}}$$

where X_{cmc} is the cmc in molar fraction, which X_{cmc}=cmc/55.4, cmc is that in mole per liter (mol/L) and was calculated by the ratio of mass concentration (grams per liter, g/L) and molecular weight (grams per mole, g/mol), and 55.4 comes from that 1 L of water corresponds to 55.4 mol of water at 25 °C. β is the degree of counterion binding to micelles. The standard enthalpy change for the micellization process,$\Delta H_{\mathrm{m}}^{0}$, can be determined using the Gibbs–Helmholtz equation:

$$\Delta H_{\mathrm{m}}^{0} = -RT^{2}(0.5+\beta)\ln X_{\mathrm{cmc}}/dT$$

Then, the standard entropy of micelle formation, $\Delta S_{\mathrm{m}}^{0}$, is obtained by the use of the following relation:

$$\Delta S_{\mathrm{m}}^{0} = \left(\Delta H_{\mathrm{m}}^{0} - \Delta G_{\mathrm{m}}^{0}\right)/T$$

The thermodynamic parameters of micellization at different temperatures for PQ are listed in Table 2. As can be seen, the Gibbs free energy ($\Delta G_{\mathrm{m}}^{0}$) are all negative, indicating that the formation of micelle is spontaneous. The values of standard enthalpy changes ($\Delta H_{\mathrm{m}}^{0}$) for micellization are negative as well, implying the micelle formation process is exothermic. The $\Delta G_{\mathrm{m}}^{0}$ values do not vary significantly upon raising the temperature; this can be understood that dispersion interactions represent the main attractive force for micelle formation. Table 2 indicate that the negative values of $\Delta G_{\mathrm{m}}^{0}$ are mainly due to the large positive of $\Delta S_{\mathrm{m}}^{0}$. $\Delta H_{\mathrm{m}}^{0}$ is much smaller than the value of $T\Delta S_{\mathrm{m}}^{0}$; therefore, the micellization process is governed primarily by the entropy gain associated with it, namely, the micellization is entropy-driven, and the driving force for the process is the tendency of the hydrophobic group of the surfactant to transfer from the solvent environment to the interior of the micelle.

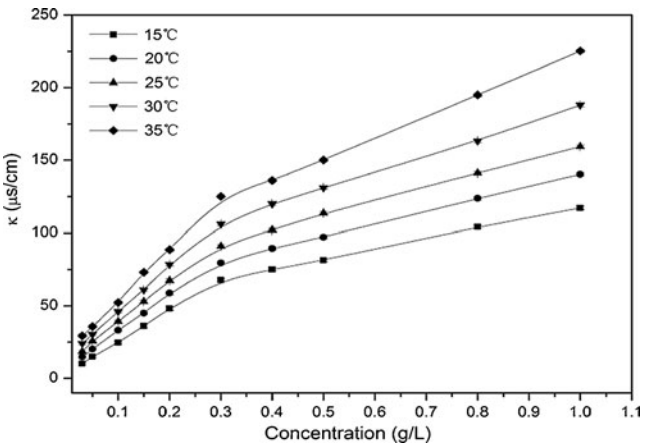

Fig. 8 Conductivity plots of the polymeric surfactant PQ in the aqueous solution at different temperatures

Table 2 Effect of temperature on parameters of micellization for PQ

Temperature °C	cmc mmol/L	cmc g/L	α	β	ΔG_m^0 kJ/mol	ΔH_m^0 kJ/mol	$T\Delta S_m^0$ kJ/mol
15	0.0224	0.29	0.32	0.68	−41.60	−20.5	21.1
20	0.024	0.31	0.34	0.66	−41.48	−10.36	31.12
25	0.0255	0.33	0.35	0.65	−41.36	−8.0	33.36
30	0.0263	0.34	0.37	0.63	−41.24	−5.48	35.76
35	0.0271	0.36	0.41	0.59	−40.55	−2.81	37.74

The effect on thermal stability of mixed system between HPAM and PQ

Figure 9 shows the relationship between the viscosity for mixed system and degradation time in the simulated water. As we can see from Fig. 9, the results represent that the viscosities of mixed system for HPAM and PQ have higher than the viscosity of HPAM, and the values of viscosity for mixed system changed a little. When the concentration of PQ is 25 mg/L, the effect of improvement for the mixed system is prior to the other concentration of PQ. When the concentration of PQ is higher than 25 mg/L, the viscosities of mixed systems reduce. In the simulated water, the high ionic strength can suppress the formation of inner salt for HPAM molecules and be in favor of the extension of molecule chains. Moreover, it helps the association of hydrophobic group parts for PQ. The presence of inorganic electrolytes also enhances the electrostatic interaction between HPAM and PQ, resulting in the increase of hydrodynamic volume and even forming a spatial network structure, so that it can increase the viscosity of the mixed solution. In a word, the mixed system for PQ and HPAM forms interaction through the static electricity force gathering electrolyte compound and increases the molecular hydrodynamic volume, so that it has also higher viscosity values and enhances the salt resistance and thermal stability of mixed system.

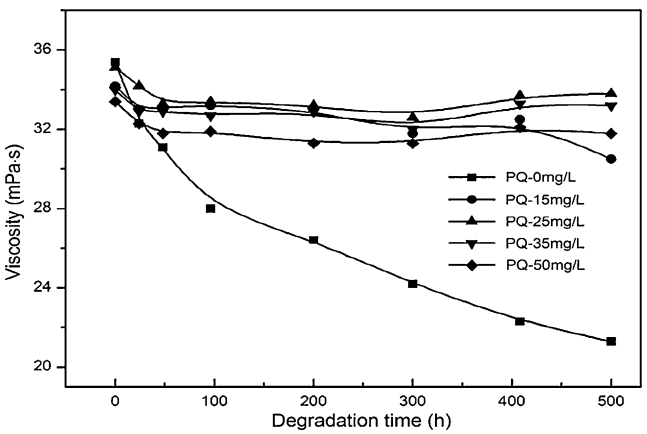

Fig. 9 Viscosity of the mixed system for HPAM and PQ at the different degradation time

Figure 10 shows the relationship between the distribution of average hydrodynamic radius and degradation time when the concentration of PQ is 25 mg/L. From Fig. 10, the distributions of average hydrodynamic radius increase first after reduce along with the extension of degradation time and the distributions of hydrodynamic radius for the mixed system are bigger than that for HPAM. During the early stages of degradation, high ionic strength combined with electrostatic interaction is conducive to the stretch of HPAM molecular chain and increases the molecular hydrodynamic volume; in the latter of degradation, the simulated temperature combined with the complexation between HPAM and highly charged cation breaks the molecular structure of mixed system, resulting in the decrease of molecular hydrodynamic volume. The results indicate that the mixed system for HPAM and PQ increases the distribution of hydrodynamic radius than single HPAM by static electricity force, which avail to the improvement of the viscosity for mixed system. This is consistent with the result of viscosity.

Conclusion

We synthesized a new PQ by cationic ring-open polymerization using trifluoride diethyl etherate as cationic catalyst. The chemical structure of PQ was ascertained by ^{1}H NMR spectrum, and the molecular

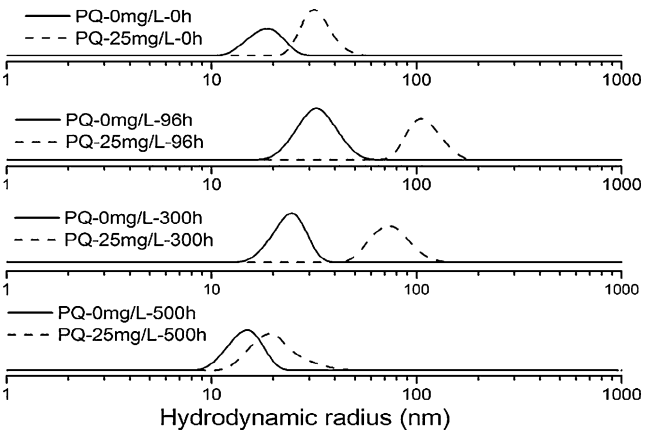

Fig. 10 Distribution of average hydrodynamic radius for the mixed system

weight of PQ is 1.292×10^4 g/mol by SLS. Surface activity and aggregation properties of PQ were studied by DLS, surface tension, conductivity, and fluorescence measurements. DLS results indicate that the distribution of the average R_h also increase as the concentrations of PQ in the aqueous solution increase. Surface tension results indicated that γ_{cmc} and cmc values of PQ decrease with increasing of sodium chloride concentration. The cmc and γ_{cmc} values of PQ measured by electrical conductivity and fluorescence measurements by and large identify with that obtained by surface tension measurements. Electrical conductivity results also show that the value of cmc rise with increasing the temperature in the aqueous solution. The thermodynamic parameters (ΔG_m^0,ΔS_m^0,ΔH_m^0) indicated that the micellization of PQ was mainly the process of entropy-driven. The results from the viscosity stability between HPAM and PQ showed that the viscosities of mixed system for HPAM and PQ are higher than the viscosity of HPAM. The viscosity stability results also suggest that the mixed system can greatly improve salt resistance and thermal stability and has the high practical application performance compared with single HPAM.

Acknowledgments The authors gratefully acknowledge the financial support from Major Research of the Ministry of Science and Technology, China (grant no. 2008zx05024-02-007) and the Scientific Research Project of Shandong Province (grant no. 2008GG2TC01011-12).

References

1. Para G, Hamerska-Dudra A, Wilk KA, Warszynski P (2010) Surface activity of cationic surfactants, influence of molecular structure. Colloids Surface Physicochem Eng Aspect 365(1–3):215–221
2. Lukác M, Pisárcik M, Lacko I, Devínsky F (2010) Surface-active properties of nitrogen heterocyclic and dialkylamino derivates of hexadecylphosphocholine and cetyltrimethylammonium bromide. J Colloid Interface Sci 347(2):233–240
3. Ao MQ, Xu GY, Pang JY, Zhao TT (2009) Comparison of aggregation behaviors between ionic liquid-type imidazolium gemini surfactant C-12-4-C(12)im Br-2 and its monomer C(12) mim Br on silicon wafer. Langmuir 25(17):9721–9727
4. Para G, Jarek E, Warszynski P (2006) The Hofmeister series effect in adsorption of cationic surfactants–theoretical description and experimental results. Adv Colloid Interface Sci 122 (1–3):39–55
5. Rosen MJ (2004) Characteristic features of surfactants. Surfactants and interfacial phenomena. John Wiley & Sons, pp 20–40
6. Yoshimura T, Yoshida H, Ohno A, Esumi K (2003) Physicochemical properties of quaternary ammonium bromide-type trimeric surfactants. J Colloid Interface Sci 267(1):167–172
7. Bell PC, Bergsma M, Dolbnya IP, Bras W, Stuart MCA, Rowan AE, Feiters MC, Engberts JBFN (2003) Transfection mediated by gemini surfactants: engineered escape from the endosomal compartment. J Am Chem Soc 125(6):1551–1558
8. Babadagli T (2003) Selection of proper enhanced oil recovery fluid for efficient matrix recovery in fractured oil reservoirs. Colloids Surface Physicochem Eng Aspect 223(1–3):157–175
9. Zana R (2002) Dimeric and oligomeric surfactants. Behavior at interfaces and in aqueous solution: a review. Adv Colloid Interface Sci 97(1–3):205–253
10. Kim SS, Zhang W, Pinnavaia TJ (1998) Ultrastable mesostructured silica vesicles. Science 282(5392):1302
11. Deen GR, Gan LH (2009) New piperazine-based polymerizable monoquaternary cationic surfactants: synthesis, polymerization, and swelling characteristics of gels. J Polymer Sci Polymer Chem 47(8):2059–2072
12. Hayamizu K, Tsuzuki S, Seki S, Ohno Y, Miyashiro H, Kobayashi Y (2008) Quaternary ammonium room-temperature ionic liquid including an oxygen atom in side chain/lithium salt binary electrolytes: ionic conductivity and 1H, 7Li, and 19 F NMR studies on diffusion coefficients and local motions. J Phys Chem B 112(4):1189–1197
13. Dopierala K, Prochaska K (2008) The effect of molecular structure on the surface properties of selected quaternary ammonium salts. J Colloid Interface Sci 321(1):220–226
14. Chlebicki J, Wegrzynska J, Wilk KA (2008) Surface-active, micellar, and antielectrostatic properties of bis-ammonium salts. J Colloid Interface Sci 323(2):372–378
15. Ao MQ, Xu GY, Zhu YY, Bai Y (2008) Synthesis and properties of ionic liquid-type Gemini imidazolium surfactants. J Colloid Interface Sci 326(2):490–495
16. Muzzalupo R, Infante MR, Perez L, Pinazo A, Marques EF, Antonelli ML, Strinati C, La Mesa C (2007) Interactions between gemini surfactants and polymers: thermodynamic studies. Langmuir 23(11):5963–5970
17. Jendric M, Filipovic-Vincekovic N, Vincekovic M, Bujan M, Primozik I (2005) Phase behavior of bis(quaternary ammonium bromide)/sodium cholate/H2O system. Journal of Dispersion Science and Technology 26(1):39–51
18. Yoshimura T, Nagata Y, Esumi K (2004) Interactions of quaternary ammonium salt-type gemini surfactants with sodium poly(styrene sulfonate). J Colloid Interface Sci 275(2):618–622
19. Kumar A, Alami E, Holmberg K, Seredyuk V, Menger FM (2003) Branched zwitterionic gernini surfactants micellization and interaction with ionic surfactants. Colloids Surface Physicochem Eng Aspect 228(1–3):197–207
20. Sikiric M, Primozic I, Filipovic-Vincekovic N (2002) Adsorption and association in aqueous solutions of dissymmetric Gemini surfactant. J Colloid Interface Sci 250(1):221–229
21. Li ZY, Chau Y (2009) Synthesis of linear polyether polyol derivatives as new materials for bioconjugation. Bioconjug Chem 20(4):780–789
22. Mortensen K (2001) PEO-related block copolymer surfactants. Colloids Surface Physicochem Eng Aspect 183:277–292
23. Mochizuki A, Senshu K, Seita Y, Fukuoka T, Yamashita S, Koshizaki N (1998) Polyether-segmented nylon hemodialysis membrane. VI. Effect of polyether segment on morphology and surface structure of membrane. J Appl Polymer Sci 69(8):1645–1659
24. Hirasaki GJ, Miller CA, Raney OG, Poindexter MK, Nguyen DT, Hera J (2011) Separation of produced emulsions from surfactant enhanced oil recovery processes. Energ Fuel 25:555–561
25. Deng ML, Cao MW, Wang YL (2009) Coacervation of cationic gemini surfactant with weakly charged anionic polyacrylamide. J Phys Chem B 113(28):9436–9440
26. Zhang HX, Xu GY, Wu D, Wang SW (2008) Aggregation of cetyltrimethylammonium bromide with hydrolyzed polyacrylamide at the paraffin oil/water interface: interfacial rheological behavior study. Colloids Surface Physicochem Eng Aspect 317(1–3):289–296
27. Khan MY, Samanta A, Ojha K, Mandal A (2008) Interaction between aqueous solutions of polymer and surfactant and its effect on physicochemical properties. Asia Pac J Chem Eng 3(5):579–585

28. Luo L, Wang DX, Zhang L, Zhao S, Yu JY (2007) Interactions between hydrophobically modified associating polyacrylamide and cationic surfactant at the water-octane interface: interfacial dilational viscoelasticity. Journal of Dispersion Science and Technology 28(2):263–269
29. Yuan SL, Cai ZT, Xu GY, Jiang YS (2003) Mesoscopic simulation study on the interaction between polymer and C12NBr or C(9) phNBr in aqueous solution. Colloid and Polymer Science 281 (11):1069–1075
30. Huang JB, Zhu Y, Zhu BY, Li RK, Fu HI (2001) Spontaneous vesicle formation in aqueous mixtures of cationic surfactants and partially hydrolyzed polyacrylamide. J Colloid Interface Sci 236 (2):201–207
31. Brackman JC, Engberts JBFN (1991) Influence of polymers on the micellization of cetyltrimethylammonium salts. Langmuir 7 (10):2097–2102
32. Turro NJ, Baretz BH, Kuo PL (1984) Photoluminescence probes for the investigation of interactions between sodium dodecylsulfate and water-soluble polymers. Macromolecules 17(7):1321–1324
33. Shirahama K, Tsujii K, Takagi T (1974) Free-boundary electrophoresis of sodium dodecyl sulfate-protein polypeptide complexes with special reference to SDS-polyacrylamide gel electrophoresis. J Biochem 75(2):309–319
34. Muller G, Fenyo JC, Selegny E (1980) High molecular weight hydrolyzed polyacrylamides. III. Effect of temperature on chemical stability. J Appl Polymer Sci 25(4):627–633
35. Del Rio E, Galià M, Cádiz V, Lligadas G, Ronda JC (2010) Polymerization of epoxidized vegetable oil derivatives: ionic-coordinative polymerization of methylepoxyoleate. J Polymer Sci Polymer Chem 48(22):4995–5008
36. Rahm M, Westlund R, Eldsäter C, Malmström E (2009) Tri-block copolymers of polyethylene glycol and hyperbranched poly-3-ethyl-3-(hydroxymethyl)oxetane through cationic ring opening polymerization. J Polymer Sci Polymer Chem 47(22):6191–6200
37. Endo T (2009) Handbook of ring-opening polymerization. Wiley-VCH Verlag GmbH & Co., pp 56,141–142
38. Magnusson H, Malmstrom E, Hult A (1999) Synthesis of hyperbranched aliphatic polyethers via cationic ring-opening polymerization of 3-ethyl-3-(hydroxymethyl)oxetane. Macromol Rapid Comm 20(8):453–457
39. Wang T-T, Iou Q-L (2002) The solvent effect and the structural effect of halides on the quaternization Et3N+RX–>Et3RNX. Chem Eng J 87(2):197–206
40. Li X, Mya KY, Ni XP, He CB, Leong KW, Li J (2006) Dynamic and static light scattering studies on self-aggregation behavior of biodegradable amphiphilic poly(ethylene oxide)-poly (R)-3-hydroxybutyrate -poly(ethylene oxide) triblock copolymers in aqueous solution. J Phys Chem B 110(12):5920–5926
41. Gracia CA, Gómez-Barreiro S, González-Pérez A, Nimo J, RodrIguez JR (2004) Static and dynamic light-scattering studies on micellar solutions of alkyldimethylbenzylammonium chlorides. J Colloid Interface Sci 276(2):408–413
42. Zimm BH (1948) The scattering of light and the radial distribution function of high polymer solutions. J Chem Phys 16(12):1093–1099
43. Zana R, In M, Lévy H, Duportail G (1997) Alkanediyl-α,ω-bis (dimethylalkylammonium bromide) 7. fluorescence probing studies of micelle micropolarity and microviscosity. Langmuir 13 (21):5552–5557
44. Weissenborn PK, Pugh RJ (1996) Surface tension of aqueous solutions of electrolytes: relationship with ion hydration, oxygen solubility, and bubble coalescence. J Colloid Interface Sci 184 (2):550–563
45. Turro NJ, Yekta A (1978) Luminescent probes for detergent solutions. A simple procedure for determination of the mean aggregation number of micelles. J Am Chem Soc 100(18):5951–5952
46. Koyanagi M (1968) Effect of dispersion forces of solventsII. On the O–O band of the near ultraviolet absorption spectrum of benzene in fluid solutions. J Mol Spectrosc 25(3):273–290
47. Ao MQ, Huang PP, Xu GY, Yang XD, Wang YJ (2009) Aggregation and thermodynamic properties of ionic liquid-type gemini imidazolium surfactants with different spacer length. Colloid and Polymer Science 287(4):395–402
48. Zana R (1996) Critical micellization concentration of surfactants in aqueous solution and free energy of micellization. Langmuir 12 (5):1208–1211
49. Nusselder JJH, Engberts JBFN (1992) Toward a better understanding of the driving force for micelle formation and micellar growth. J Colloid Interface Sci 148(2):353–361